ISBN number: 978-1-925627-66-4

Please select category below:
Normal Paper ☒
Student Paper ☐
Young Engineer Paper ☐

Accelerated Gearbox Degradation Monitoring using a Combination of Vibration and Acoustic Emission Features

Cristobal Ruiz-Carcel [1], Andrew Starr [1]

[1]*Cranfield University, Cranfield, Bedfordshire MK430AL, United Kingdom*

Abstract

Commercial HUM systems usually rely on vibration measurements to assess the condition of shafts, gears, and bearings in rotorcraft transmission systems. Recent research has shown that acoustic emissions (AE) can be advantageous in the detection of mechanical faults in helicopter gearboxes. In particular AE has been successful in detecting very early small defects on bearings and gears, increasing sensitivity during the fault detection process and providing extra time for maintenance planning. Additionally, knowledge about the gear degradation process can be used to define rules that combine AE and vibration sensing technologies, adding robustness to the fault detection process by minimising false alarms.
In this study, a mixture of AE and vibration signal features were used to monitor accelerated natural degradation in an experimental gear rig. The suggested signal processing technique first defines individual alarm levels for each feature based on statistical analysis of the signals during healthy operation. Then proposes knowledge-based rules to merge them into a single health indicator for fault detection. This combined approach has the benefit of producing an early fault warning, and increases the confidence in the fault detection procedure as the features reach threshold values systematically, reducing the chances of false alarms.

Keywords: acoustic emission, vibration, feature extraction, natural degradation, data fusion

1. Introduction

Health and Usage Monitoring Systems (HUMS) typically use predefined vibration features to assess the condition of rotorcraft transmission systems [1]–[3]. Commercial HUMS make use of different vibration analysis methods to detect faults in bearings, gears and shafts. Condition Indicators (CI's) are key vibration features extracted from the acquired vibration signals, which can be related to specific mechanical faults [4]. In HUMS a range of different CI's are extracted from vibration data to characterize component health.

Acoustic emissions (AE) are defined in the field of machine monitoring as transient elastic waves produced by the interface of two components or more in relative motion [5]. Typical AE sources include impacts, crack growth, friction, turbulence, material loss, cavitation, leakage etc. Its main benefit against vibration analysis and oil analysis is the capability to detect faults earlier due to the high sensitivity offered by AE [6]. On the other hand, the main drawback of AE is the difficulty in processing, interpreting and manipulating the acquired data [7], [8]. Vibration-based gearbox monitoring is well established, however the application of AE to this field is still in its early stages [6], [9] and it is difficult to see it implemented in commercial tools. In the area of HUMS some research has been carried out in recent years to prove the

capabilities of AE to monitor helicopter transmission components[10]–[12]. These investigations concluded that AE offered much earlier indication of damage than vibration analysis, and the proposed processing techniques were suitable for gearbox fault diagnosis.

Combination of multiple features from multiple sensors has the advantage of improving the effectiveness of fault detection, as different features are sensitive to different faults or degradation stages. However, such combinations can lead to oversensitive systems, as the random variations inherent to each indicator are combined, false alarms would be triggered often if the CI's are not processed properly. Currently, data fusion techniques are used to tackle this problem, frequently relying on machine learning methods to produce sensitive and robust CI's [13]. Despite the success of these techniques, it is difficult to interpret the data manipulation that they produce as they act as black-box algorithms. Consequently, its implementation is still an issue in highly regulated and safety critical industries such as aerospace, which require traceability in the data processing. For that reason, the proposed data fusion approach first defines individual alarm levels for each feature based on statistical analysis of the signals during healthy operation. Then proposes simple and traceable rules based on degradation and failure knowledge to merge them into a single health indicator for fault detection. This combined approach has the benefit of producing early fault warnings, and increases the confidence in the fault detection procedure as the features reach threshold values systematically, reducing the chances of false alarms.

2. Methodology

2.1 Sensing

The iNDTact GmbH iMPactXS acoustic emission sensor (frequency range 0.1 Hz to 1MHz) was used for AE monitoing. It was connected to an iNDTact champ charge amplifier and a PicoScope 4224 IEPE digital oscilloscope was used to digitise the signal at 2 MHz to meet the Nyquist criterion. A triaxial accelerometer Brüel & Kjaer 4535-B (frequency range of 0.3 to 10 kHz in X and Y axes, and 0.3 to 12.8 kHz in Z) was selected for vibration monitoring. Vibration signals were sampled at 51.2 kHz using a National Instruments 9234C data acquisition card. Both sensors were installed in a compact machined aluminium block (Figure 3). Other rig sensors include an induction sensor to provide a once per rev signal in the input shaft, output shaft speed sensor, torque measurement in the dynamometer and oil sump temperature.

2.2 Experimental setup

The instrumented rig used to generate the data is a single stage gearbox rig (Figure 1) powered by an 11kW induction motor with 2 pairs of poles, and a nominal speed of 1490 rpm. The output shaft is connected to a dynamometer that absorbs and measures the load applied. The gear pair has straight teeth, a module of 5, and 24 and 25 teeth in the input and output shafts respectively. A lubrication port on the gearbox casing cover provided lubrication from an external pump. Although this benchtop arrangement is quite different from a helicopter gearbox in terms of shape, size, power, and stiffness, the gear meshing dynamics are the same as in any gear pair. The transmission path for the fault generated forces through the gears, shafts, and bearings to the static components is also comparable. Figure 2 shows a detail of the gear pair. Figure 3 shows the sensor cluster installed in the vicinity of the input shaft bearing housing.

2.3 Testing procedure

Data from both sensors, as well as speed, torque and temperature measurements were acquired. For simplicity, only the Z axis vibration signal was considered. The dynamometer was set to a

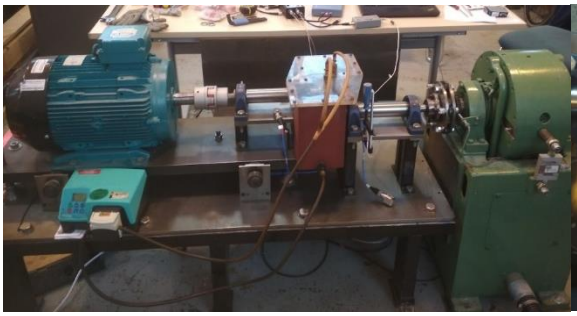

Figure 1: Gear rig

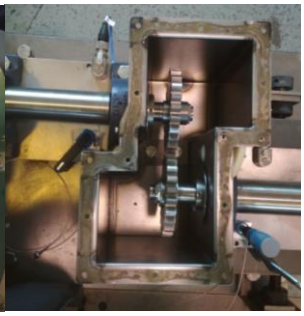

Figure 2: Gear pair

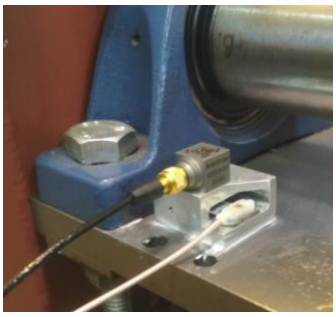

Figure 3: Sensor location

constant value of 30Nm. Vibration data was acquired in recordings of 1s (covering around 24 revolutions), while the broadband sensor data recordings lasted 0.2s to keep a reasonable volume of data due to high sampling rate. Observations were acquired in intervals of 30 seconds.

Although the gear rig was originally designed using EN24T alloy steel for infinite life, a softer gear manufactured in EN8 mild steel was used in the output shaft to accelerate pitting degradation to study the evolution of the CI's in a reasonable amount of time. This failure mode was selected as planetary gear sets are more vulnerable to pitting defects due to intricate lubrication conditions. With the increase of the running cycles, the micro pitting will induce more deleterious faults, such as spalling and chipping [14]. The test was run continuously, stopping every 30 minutes to observe the state of the gear and take photographs for reference. An initial run-in period of 2 hours was not considered in the analysis. The test ended when severe degradation in the form of pitting and tooth face deformation was observed.

2.4 Signal processing strategy

After the anti-aliasing filter and digitation, the vibration signals were processed directly for feature extraction. The AE signals were high-pass filtered after preamplification and digitation. This multi-sensor approach allows for independent analysis of "low frequency" vibration-like events (such as oscillations related to misalignment, unbalance, gear mesh, bearing faults or resonances) from "high frequency" events such as impacts, friction or crack growth. Gear specific features based on statistical moments of time synchronous average (TSA) and its derivatives (difference and residual signals) were also computed. The features extracted from acquired signals are represented in Table 1, which shows a mixture of time domain, frequency domain, and gear specific condition indicators. Details of the calculation of these CIs can be found in [15].

Table 1: Features extracted

AE	Vibration		
	Time domain	Frequency domain	Gear specific
1) RMS 2) CF 3) K 4) Peak count	5) RMS 6) CF 7) K	8) Shaft speed (1X) 9) 2x Shaft speed (2X) 10) GM 11) 2xGM 12) Sidebands around GM (GM ±1X) 13) Energy in 4-7 KHz range	14) FM4 15) M6A 16) M8A 17) FM0 18) Energy Ratio 19) Na4

The selection was based on well-known robust features that are sensitive to the different stages of degradation. For instance Kurtosis (K), sidebands around the gear mesh (GM) frequency or energy in the 4-7 kHz region were selected to be sensitive to resonances excited by small impacts as the gear teeth surface starts to degrade. GM frequency and harmonics amplitude is expected to rise as degradation progresses. Overall signal features such as RMS or Crest Factor

(CF) are known for not being too sensitive to early stages of degradation, but are expected to rise with mechanical looseness and ancillary damage. AE feature extraction is based on basic time domain features including RMS, CF and K. Additionally, AE peak count was obtained as the number of points exceeding the threshold value, above background noise levels (0.3V).

The probability density function of each CI was estimated using Kernel density estimation [16] to set the threshold values that differentiates between healthy (green) and degradation (yellow) state. Subsequently, the threshold was set using a confidence bound of 90%. A second threshold was used to determine the limit between the degradation stage and critical failure (red). As this threshold would typically require failure data that is rarely available in real life, a value of 1.5 times the first threshold was used for simplicity. Once the data was classified in these 3 categories using the estimated thresholds, a moving window was used to eliminate alarms produced by random variations, under the assumption that once a certain degradation mechanism starts, it cannot be reverted. Hence a new higher degradation category can only be reached when at least 5 observations in a moving window of 10 samples have reached a higher state. Under the same assumption, once a state is reached in a CI, it cannot go down again.

The data fusion rules aim to combine all the extracted CIs into one single health indicator. In this case, it proposes 4 different health states: healthy system (dark green), degradation started but not confirmed (clear green), degradation confirmed (yellow), and critical state (red). The reasoning behind this is that the non-confirmed degradation can be used to inform the maintenance crew to follow closely the case, but not necessarily to inform the pilot in real time as the fault may be in the very early stages of degradation and does not require immediate action. That prevents unnecessary worries and adds confidence on the information provided by the condition monitoring system, as it only rises alarms that are confirmed by different indicators triggered systematically as expected from gear degradation knowledge. AE indicators can only trigger the transition from healthy to degradation, as they are very sensitive to incipient faults. Subsequently, the degradation needs to be confirmed by changes in key frequency CI's, or impact sensitive CIs (K). Critical state has to be confirmed by overall vibration levels increased (RMS, CF).

3 Results and discussion

3.1 Gear degradation observed

Figure 4 shows the observed changes at different points of the experiment. The brand new gear had some minor marks and scuffs in the axial direction from the manufacturing process. After 2 hours of run-in, the teeth contact surfaces were smoothly polished. That was considered the starting point of the test. Four hours later, some minor pitting marks were observed in the central area of the contact surfaces. As the test progressed, the amount of pitting observed grew, initially expanding laterally and later affecting most of the contact surface. After 10 hours of testing, in addition of generalised pitting, a significant amount of material had disappeared from the central area of the contact surface. That was considered as the point where damage reached a critical level. Thirteen hours into the test damage in the contact surfaces was severe, the original involute profile was completely distorted, and deformation in the axial direction appeared. The test was stopped at this point to avoid damage in the rig.

3.2 Signal analysis results

Figure 5 (top) shows the results obtained for the 19 CI's extracted after applying the thresholding method described in 2.4. The 4 hours of test after the run-in period were considered

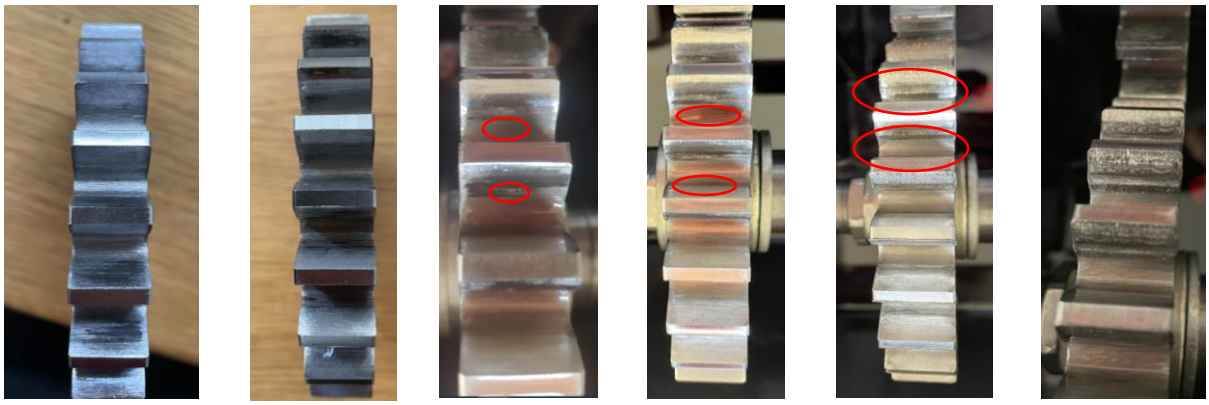

New | After run-in | After 4 hours | After 6 hours | After 10 hours | After 13 hours

Figure 4: Gear degradation observed

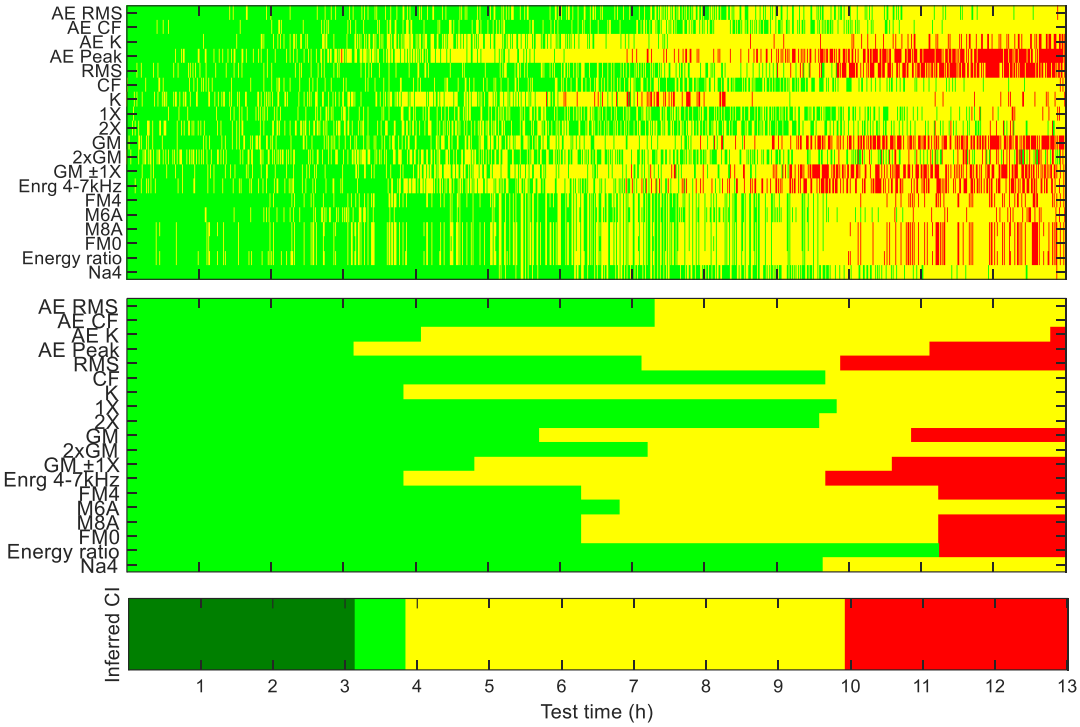

Figure 5: Computed CI's; after thresholding (top), after moving window (middle), inferred health state (bottom)

healthy operation, as no surface damage was observed. This period was used to obtain the threshold value for each CI. As shown in Figure 5 (top), around 10% of the observations in this period are classified as damaged (yellow), as expected from the 90% confidence bound used in the analysis of each probability density function. The moving window approach in Figure 5 (middle) gets rid of these false alarms, and produces monotonic CI's. The first CI to consistently reach a value above the threshold is the AE peak count, around 3.2h after the start of the experiment. That moves the rule-based inferred health state from healthy to "fault detected but not confirmed" (clear green) state. The next indicator to reach a consistent yellow value is energy in the 4-7 kHz region around 3.85 h into the experiment, confirming the presence of the fault and changing the state of the inferred CI. Other indicators such as K, GM and some gear specific indicators are triggered later, further confirming the fault detection. The first indicator to consistently reach the critical state is energy in the 4-7 kHz range around 9.6h into the test, but according to the rules' logic, the inferred CI moves to critical state when RMS reaches critical values after 9.9h, indicating overall increased levels of vibration. The inferred health state obtained using rules based on gear damage and signal processing knowledge is consistent with the observations during the test, and only uses statistical analysis from healthy data for threshold estimation.

4 Conclusion

The use of multiple sensors and multiple condition indicators can enhance the sensitivity of a fault detection system, as it allows the detection of different physical phenomena as the fault progresses. However, this approach complicates the interpretation of the data, and often it is required to merge the CI's to give the user concise but yet precise information. Using logical rules based on engineering knowledge about degradation mechanisms can provide a simple but reliable and traceable way of solving that issue. The results obtained in this study using accelerated gear degradation data from AE and vibration measurements show how damage alarms are triggered systematically during the different stages of degradation, and how the rules proposed provide an inferred CI that is reliable and robust. Future work will look into further signal pre-processing to account for changes in operating conditions (speed, torque, temperature, etc.) and compare the performance of simple rule-based CI combination approaches with state of the art data fusion algorithms.

ACKNOWLEDGEMENT

This research has received funding from the Clean Sky 2 Joint Undertaking under the European Union's Horizon 2020 research and innovation programme under grant agreement No 738144.

REFERENCES

[1] J. Zakrajsek, D. Townsend, and H. Decker, "An Analysis of Gear Fault Detection Methods as Applied to Pitting Fatigue Failure Data," Feb. 1993.

[2] J. Zakrajsek, D. Townsend, D. Lewicki, H. Decker, and R. Handschuh, "Transmission Diagnostic Research at NASA Lewis Research Center," p. 14, Nov. 1995.

[3] H. Decker, "Crack Detection for Aerospace Quality Spur Gears," p. 15, Apr. 2002.

[4] P. Dempsey, J. Keller, D. Wade, and R. Arsenal, *Signal Detection Theory Applied to Helicopter Transmission Diagnostic Thresholds*. 2008.

[5] D. Mba and R. B. K. N. Rao, "Development of acoustic emission technology for condition monitoring and diagnosis of rotating machines: Bearings, pumps, gearboxes, engines, and rotating structures," *Shock and Vibration Digest*, vol. 38, no. 2, pp. 3–16, 2006,

[6] C. K. Tan, P. Irving, and D. Mba, "A comparative experimental study on the diagnostic and prognostic capabilities of acoustics emission, vibration and spectrometric oil analysis for spur gears," *Mech Syst Signal Process*, vol. 21, no. 1, pp. 208–233, Jan. 2007, doi: 10.1016/J.YMSSP.2005.09.015.

[7] A. M. Al-Ghamd and D. Mba, "A comparative experimental study on the use of acoustic emission and vibration analysis for bearing defect identification and estimation of defect size," *Mech Syst Signal Process*, vol. 20, no. 7, pp. 1537–1571, Oct. 2006, doi: 10.1016/J.YMSSP.2004.10.013.

[8] J. Couturier and D. Mba, "Operational bearing parameters and acoustic emission generation," *Journal of Vibration and Acoustics, Transactions of the ASME*, vol. 130, no. 2, 2008,

[9] Y. Qu, B. van Hecke, D. He, and J. Yoon, "Gearbox Fault Diagnostics using AE Sensors with Low Sampling Rate," vol. 31, pp. 67–90, 2013.

[10] F. Elasha, M. Greaves, D. Mba, and D. Fang, "A comparative study of the effectiveness of vibration and acoustic emission in diagnosing a defective bearing in a planetry gearbox," *Applied Acoustics*, vol. 115, pp. 181–195, Jan. 2017, doi: 10.1016/J.APACOUST.2016.07.026.

[11] F. Duan, F. Elasha, M. Greaves, and D. Mba, *Helicopter Main Gearbox Bearing Defect Identification using Vibration and Acoustic Emission Techniques*. 2015. doi: 10.1109/ICPHM.2016.7542856.

[12] A. Qu, B. Hecke, D. He, J. Yoon, E. Bechhoefer, and J. Zhu, "Gearbox Fault Diagnostics using AE Sensors with Low Sampling Rate," *Journal of Acoustic Emission*, vol. 31, pp. 67–90, Jan. 2013.

[13] A. Tsanousa *et al.*, "A Review of Multisensor Data Fusion Solutions in Smart Manufacturing: Systems and Trends," *Sensors*, vol. 22, no. 5. MDPI, Mar. 01, 2022. doi: 10.3390/s22051734.

[14] Y. Huangfu, X. Dong, K. Chen, G. Tu, X. Long, and Z. Peng, "A tribo-dynamic based pitting evolution model of planetary gear sets: A topographical updating approach," *Int J Mech Sci*, vol. 220, p. 107157, Apr. 2022, doi: 10.1016/J.IJMECSCI.2022.107157.

[15] P. Samuel and D. Pines, "A review of vibration-based techniques for helicopter transmission diagnostics," *J Sound Vib*, vol. 282, pp. 475–508, Apr. 2005, doi: 10.1016/j.jsv.2004.02.058.

[16] P.-E. P. Odiowei and Y. Cao, "Nonlinear dynamic process monitoring using canonical variate analysis and kernel density estimations," *IEEE Trans Industr Inform*, vol. 6, no. 1, pp. 36–45, 2010,